HARRY A. C. EATON

MAGNETIC NERVE STIMULATION

Magnetic nerve stimulation is a noninvasive, noncontact means of exciting nerves. Magnetic stimulators generate eddy currents in tissue by producing a high-amplitude, short-duration magnetic pulse from a small coil located near the tissue. A simple circuit can generate the large coil currents necessary for magnetic nerve stimulation. Careful selection of circuit components is necessary to control the influence of parasitic elements on the stimulus. The spatial distribution of the induced electric field is computed for a simple model system excited by a circular coil. Surface charges are induced at tissue boundaries and significantly affect the total induced field.

INTRODUCTION

Artificial stimulation of muscle and nerve tissues has many applications in both clinical medicine and biological research. Electrodes in contact with the body are normally used to apply an electric field within the tissue medium that can excite these tissues. An electric field may also be induced in the tissue by a time-varying magnetic field. The term "magnetic stimulation" is generally used to describe this technique. Magnetic stimulation has several advantages compared with conventional electric stimulation. The magnetic field will penetrate bone without attenuation, allowing painless stimulation of the brain through the intact head.[1] This fact has led to considerable interest in magnetic stimulation in recent years. Magnetic stimulation does not require contact between the stimulator and subject, and no surface preparation is necessary. Some disadvantages to magnetic stimulation include difficulty in stimulating only a small target and difficulty determining the exact site of stimulation.[2] Magnetic stimulation requires very large magnetic-field pulses, making the wave shape of the induced field difficult to adjust. Also, the electronics used by magnetic stimulators are quite bulky compared with those of conventional stimulators.

Magnetic stimulation is approved by the Food and Drug Administration for use on peripheral nerves in humans but not for brain stimulation. Nonetheless, many investigators have obtained exemptions for investigational devices to explore the potential for brain stimulation. Some clinically useful results from magnetic brain stimulation include measuring central motor conduction time in the early diagnosis of multiple sclerosis[1,3,4,5] and monitoring efferent pathways in the spinal cord during spinal surgery.[6,7] Some exploration into the cognitive functioning of the brain has also been performed with magnetic stimulation. Examples include evidence of motor program storage in the motor cortex,[8] estimation of letter recognition processing time in the visual cortex,[9] and demonstration of a sense of movement in missing limbs of amputees.[10] Peripheral nerve stimulation has also been shown to be effective for several clinical uses, including stimulating the facial nerve,[11,12] lumbosacral roots,[13,14] and phrenic nerve.[15] Because of the poor localization of magnetic stimulators, they are not suitable for routine electrodiagnostic use on peripheral nerves.[16]

STIMULATOR CIRCUIT

The Laboratory has developed a magnetic stimulator capable of producing rapid stimulating pulse trains (see Fig. 1). This instrument uses a custom-designed switch-mode power supply with active power-factor correction. The power supply rapidly charges a capacitor bank, which is then discharged through the stimulating coil. The time-varying magnetic field is generated by short-duration, large-amplitude current pulses delivered to a coil located near the target tissue.

Figure 2 shows a simple circuit used for magnetic stimulation. The resistors, r_1 and r_2, in the figure represent parasitic resistances of the circuit and are not inten-

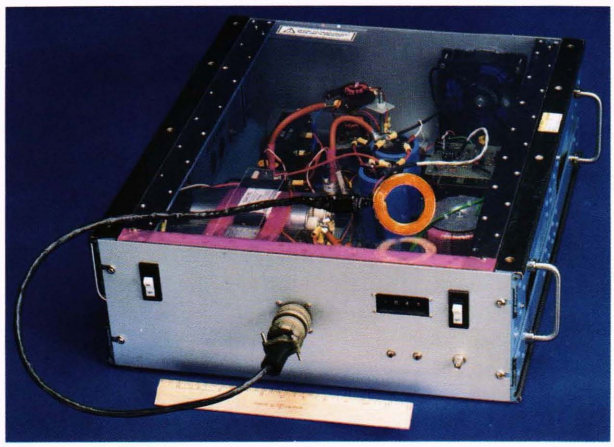

Figure 1. A photograph of the APL-designed magnetic stimulator. A six-turn round coil is shown connected to the stimulator. The coil is placed next to the target tissue when the current pulse is initiated.

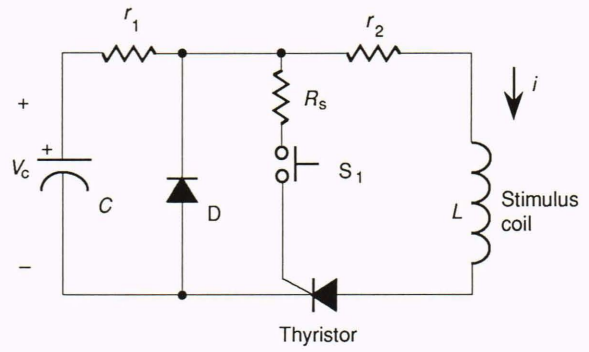

Figure 2. A simplified schematic of a magnetic stimulator circuit. C is the capacitor; V_c is the capacitor voltage; r_1 represents the internal series resistance of the capacitor; r_2 represents the equivalent series resistance of all components to the right of the diode (D); R_s is the resistor used to limit the trigger current; S_1 is the trigger switch; the inductor L is the stimulus coil and will be located near the target tissue; i is the current through the stimulator coil. A circuit that initially charges the capacitor is necessary, but not shown.

tionally added. Figure 2 omits the charging circuit necessary to produce the initial charge on the capacitor. A solid-state thyristor discharges the capacitor into the coil. The trigger circuit shown is for illustration only; the operator's switch would normally be isolated from the high-energy circuit.

After the switch, S_1, is pressed, the thyristor is triggered, allowing the capacitor to discharge through the coil. Current will flow through the capacitor until the voltage at the capacitor terminals reaches zero. During this time, the coil current i can be described by a series resistor–inductor–capacitor (RLC) circuit equation (treating the thyristor as an ideal switch):

$$i(t) = \frac{V_c \sin\left\{t\sqrt{(1/LC) - [(r_1 + r_2)/2L]^2}\right\}}{\sqrt{(L/C) - [(r_1 + r_2)^2/4]}}$$

$$\times \exp\left[-\frac{t(r_1 + r_2)}{2L}\right], \qquad (1)$$

where V_c is the initial capacitor voltage, t is the time passed since the trigger switch was pushed, L is the inductance of the stimulator coil, and C is the capacitance. This equation is valid for the time interval from $t = 0$ (when the thyristor is triggered) until time $t = t_s$ when the diode begins to conduct. If the diode is assumed ideal, then t_s is given by

$$t_s = \frac{\tan^{-1}\left\{\dfrac{2L\sqrt{(1/LC) - [(r_1 + r_2)/2L]^2}}{r_1 - r_2}\right\}}{\sqrt{(1/LC) - [(r_1 + r_2)/2L]^2}}. \qquad (2)$$

Equation 2 uses a four-quadrant arctangent function. The time, t_s, is slightly later than the time at which the current is maximal. After t_s, the current circulates through the diode, thyristor, and coil and is governed by a series resistor-inductor (RL) circuit equation (again assuming ideal diode and thyristor behavior):

$$i(t > t_s) = I_s \exp\left[-\frac{(t - t_s)r_2}{L}\right], \qquad (3)$$

where I_s is the coil current at the time that the diode begins to conduct and is given by

$$I_s = \frac{V_c \exp[-t_s(r_1 + r_2)/2L]}{\sqrt{(L/C) - r_1 r_2}}. \qquad (4)$$

Resistance r_2 is normally dominated by the coil resistance. That resistance is frequency dependent because of the skin effect unless special construction techniques are used for the coil. The AC resistance near the ringing frequency is used for r_1 and r_2 in all equations except Equation 3. The DC resistance is used for r_2 in Equation 3; using the DC value neglects the frequency content of the exponential decay but gives reasonable answers. In addition, the equations neglect the stray inductances of the capacitor, diode, and thyristor, as well as those of their wiring (the coil cable inductance may be added to the coil inductance); nonetheless, they provide good first-order results.

The APL-designed magnetic stimulator utilizes a circuit similar to that shown in Figure 2. The capacitor is 250 μF, r_1 is 0.005 Ω, r_2 is 0.046 Ω at 5 kHz and 0.022 Ω at DC, and the coil inductance is 3.5 μH. Figure 3 shows an oscilloscope recording of the coil current and the induced electric field measured at a point 1.5 cm above the coil annulus for an initial capacitor charge of 845 V. The peak current is 5.3 kA; that level is reached about 45 μs after the start of the pulse. Slight ringing is observed when the current switches from the capacitor to the diode because of stray inductances in the capacitor and diode circuits.

The capacitor stores considerable energy (89 J in the preceding example), most of which is dissipated as heat in the coil resistance. After several pulses have been delivered to the coil, its temperature will rise appreciably. The temperature elevation increases the coil resistance, which will reduce the peak current of subsequent pulses. Sufficient time should be allowed between pulses or pulse trains to allow the coil to cool.

SPATIAL DISTRIBUTION OF INDUCED FIELD

The excitation threshold of a nerve fiber is a strong function of the spatial distribution of the applied electric

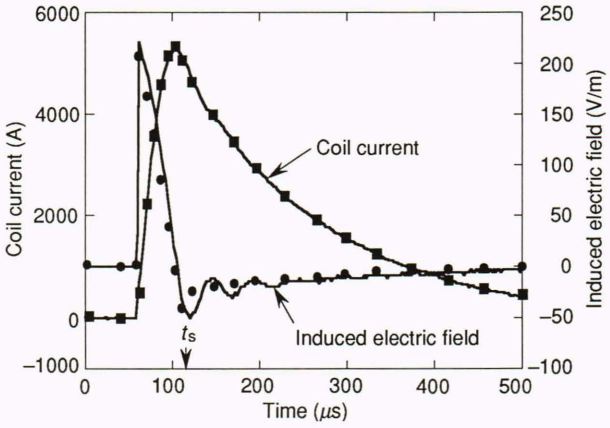

Figure 3. An oscilloscope recording of the coil current and induced electric field in a saline-filled beaker. Solid lines are measurements; symbols are theoretically computed values. The positive and negative areas of the induced electric field are equal because the coil current begins and ends at zero. The time at which the diode switches on, t_s, is given by Equation 2.

field.[17] The spatial distribution of the induced field from a magnetic stimulator is a function of the coil geometry and placement, as well as of the shape and electrical characteristics of the body.

The frequencies used for magnetic stimulation are quite low (1 to 10 kHz). The resulting wavelengths and skin depths are very large in weakly conducting materials, such as those found in the body. All practical magnetic stimulators use coils that are much smaller than a wavelength, and the target tissues are much less than one wavelength away from the coil. These properties allow for a quasi-static analysis that neglects propagation and skin effects.[18] Given these assumptions, the magnetic field can be found from the curl of a magnetic vector potential, where the vector potential is given by

$$\mathbf{A} = \mu_0 \oint_{\text{coil}} \frac{i\, d\mathbf{l}}{4\pi R}, \tag{5}$$

where μ_0 is the permeability of free-space, R is the distance between the differential element of the coil wire and the point in the body where $\mathbf{A}$ is being computed, and $d\mathbf{l}$ is directed along the path of the current. The vector integration in Equation 5 must be done with rectangular components. The current in the stimulator coil is assumed to be flowing in negligibly small filaments. The expression for $\mathbf{A}$ will have zero divergence because the coil current forms a closed loop. The current path along the cable from the coil to the capacitor bank can be neglected if the cable is of a coaxial type or has low inductance. It can be shown that the induced electric field can be found from the negative time derivative of the magnetic vector potential minus the gradient of a scalar potential V:

$$\mathbf{E} = -\mu_0 \frac{di}{dt} \oint_{\text{coil}} \frac{d\mathbf{l}}{4\pi R} - \nabla V\ . \tag{6}$$

The ∇V term arises from the charge density appearing on the boundaries, at interfaces between different tissues, or at other inhomogeneities. In a homogeneous, isotropic medium, either of infinite extent or having appropriately symmetrical boundaries for the coil under consideration, the charge density will be zero and, consequently, only the integral term in Equation 6 contributes to the electric field.

The potential function V is found from considerations of the currents at the interfaces, on the boundaries, and at inhomogeneities. In any region, $\mathbf{E}$ must satisfy

$$(\sigma\nabla \cdot \mathbf{E}) + (\mathbf{E} \cdot \nabla\sigma) = \epsilon \frac{\partial}{\partial t}(\nabla \cdot \mathbf{E}) - \left(\frac{\partial \mathbf{E}}{\partial t} \cdot \nabla\epsilon\right). \tag{7}$$

In a homogeneous region (where the permittivity ϵ and conductivity σ do not vary spatially), $\nabla\epsilon$ and $\nabla\sigma$ vanish, leading to an exponential decay of $\nabla \cdot \mathbf{E}$ and hence of charge density. Because the integral term in the expression for $\mathbf{E}$ already has zero divergence, $\nabla^2 V$ must equal zero (Laplace's equation) in a homogeneous region. In nonhomogeneous regions and on the boundaries of homogeneous regions, V must be computed so that $\mathbf{E}$ satisfies Equation 7. Equation 7 leads to Neumann-type boundary conditions for a homogeneous region. Charges will build up at the boundary of a homogeneous region in response to the applied field. For most purposes, the boundary conditions used to determine V can be computed for the steady-state case when $di/dt = 1$, and the result is multiplied by di/dt. Using the steady-state condition neglects the $\partial\mathbf{E}/\partial t$ terms in Equation 7. Omitting these terms neglects the time lag between the application of the field and the resultant rearrangement of charge; however, even the most capacitive biological materials have charge relaxation times of less than 250 ns. The result of this simplification is that the spatial distribution of the field does not vary with time.

The electric field of Figure 3 was measured with a coaxial probe having an exposed center conductor 0.56 cm long. A beaker filled with 0.9% saline solution was placed over the coil in an axially symmetric fashion. For this geometry, the boundary conditions are met by symmetry, and V is identically zero. The electric field was computed from Equation 6, where the current was found from Equations 1 through 4. Each turn of the six-turn coil (inner diameter 4.4 cm, outer diameter 7.1 cm) was integrated separately. The coil was toroidally wound with a ground wire to provide Faraday shielding to eliminate any capacitive pickup by the probe. The computed field has about 8% lower amplitude than the measured field. The scaling error may arise from the perturbation introduced by the presence of the measurement probe in

the solution. The ringing in the measured induced field is caused by the slight ringing in the coil current described previously. The induced field follows the time derivative of the coil current, so the high-frequency ringing is enhanced in the electric field.

Equation 6 can be used to predict the induced electric field inside homogeneous conductors having simple shapes for nearly any practical coil arrangement. A crude model for the head is that of a uniform spherical conductor. Figure 4 shows the electric field inside a spherical

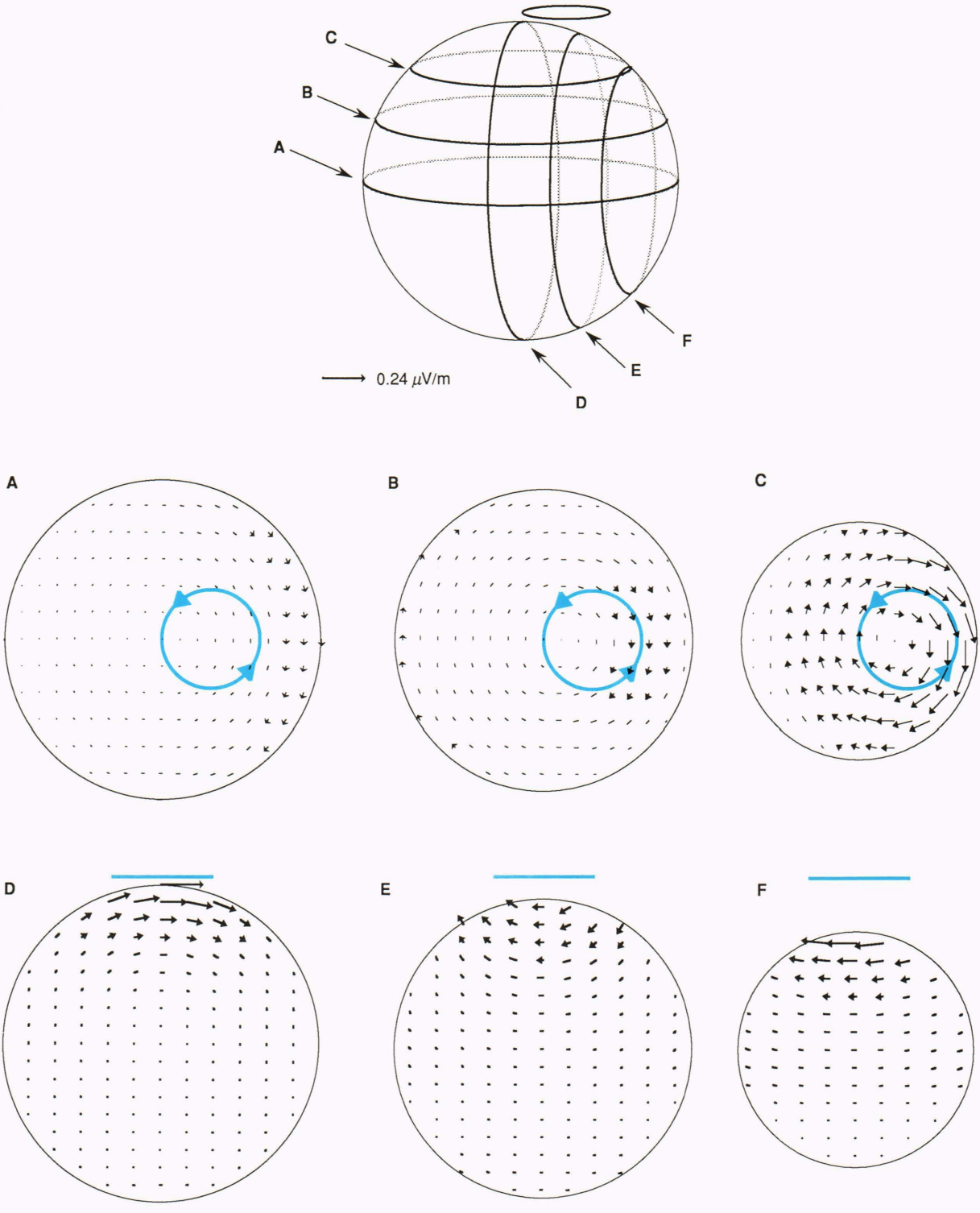

Figure 4. The induced electric field in a spherical volume conductor from a round coil placed off-center. The vectors shown in slices A through F in the bottom part of the figure indicate electric field magnitude and direction of the in-plane component. The tail of each vector is located at the point where the computation is made. Arrowheads are omitted from very short vectors. The electric field amplitude is scaled by the time derivative of the coil current. The projection of the coil is shown in blue.

volume conductor bounded by an insulator. The conducting sphere has a diameter of 18 cm. A circular one-turn coil 5 cm in diameter is located 0.3 cm above the sphere. The coil plane is tangent to the sphere surface, and the coil edge is located directly above the center of the sphere. This arrangement is shown in Figure 4. The vector potential was found by using numerical integration. An analytical solution to the scalar potential was found as a function of the vector potential for this geometry. The induced electric fields through several planar slices of the sphere are shown in the figure. Slices A and D include the sphere center, while the others are parallel and spaced 3.0 cm apart. The vectors point in the direction of the electric field, and their tails are located at the site where the field is computed. The length of the vector represents the magnitude of the in-plane component of the electric field. Arrowheads are omitted from very short vectors. The scale factor for the vectors is normalized with respect to di/dt.

Figure 4 shows that the electric field is generally stronger at locations close to the coil winding. The off-center coil placement produces boundary effects that increase the field strength near the right-hand edge of the sphere (easily seen in slice C). On the right-hand side of the sphere, the field strength does not decrease with depth (from the coil) nearly as quickly as it does in the center (compare F with D). The result is that strong electric fields of similar magnitude are found in two widely separated locations, even though the coil winding is near the sphere at only one point. This finding suggests that magnetic stimulation of the brain by a coil oriented like that shown in Figure 4 might cause stimulation at two widely spaced sites.

PHYSIOLOGICAL EXPERIMENTS

The APL-designed magnetic stimulator is being used to investigate the mechanisms of magnetic nerve stimulation. Interactions between induced fields and nerve tissue are not well understood, particularly in the brain. Induced field equations have recently been combined with simple nerve cable models to investigate these interactions.[18,19] Very little experimental evidence currently available applies to the model predictions because the models describe the behavior of single fibers, and most experiments measure compound potentials. A series of experiments is under way to examine some of the predictions from these models. Figure 5 shows an action potential measured *in vivo* from a single large-diameter nerve fiber in a monkey peripheral nerve. Teased fiber techniques and action potential collisions were used to demonstrate single-fiber recording.[20] Recordings were made from a dissected portion of the nerve in the upper arm. The threshold for producing an action potential in this fiber was a peak coil current of 4.2 kA.

The APL magnetic stimulator has also been used to stimulate a dog's brain *in vivo* through the intact skull. A compound action potential was measured with an epidural electrode in the spinal cord. Stimuli were provided at a rate of 3.5 pulses per second, and thirty recordings were averaged. A large stimulus artifact observed in the recording was caused by the voltage induced in the electrode cables. A 5-cm shift in coil location eliminated the compound action potential but did not affect the stimulus artifact.

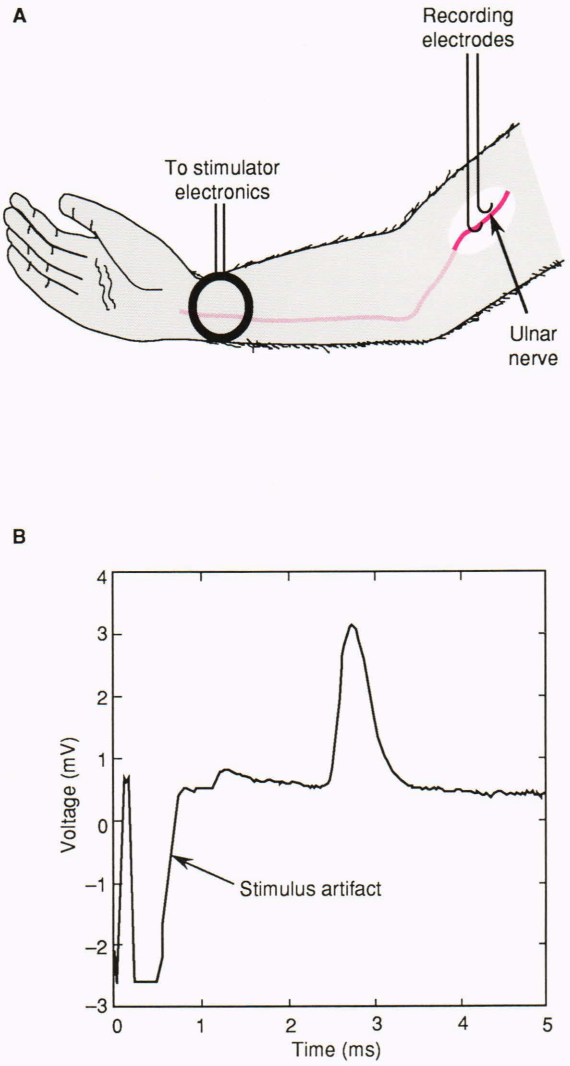

Figure 5. An experiment in the arm of a monkey to determine magnetic stimulation threshold. **A.** The experimental setup showing coil placement and recording preparation. **B.** An action potential recorded from a single myelinated peripheral nerve. Threshold stimulation was achieved at a peak coil current of 4.2 kA. A stimulus artifact appears at the beginning of the trace. Special care was taken to minimize the stimulus artifact so that the action potential is undistorted.

CONCLUSION

Magnetic stimulation is a promising new technique for stimulating excitable tissues. It offers many advantages over the use of electrodes in some applications. Recent advances have produced good focalization of stimulation in the human brain; selective stimulation of motor areas for each finger in the hand has been reported.[21] As the interaction between nerves and fields becomes better understood, new coil designs should emerge that will further improve magnetic stimulation techniques.

REFERENCES

[1] Baker, A. T., Freeston, I. L., Jalinous, R., and Jarratt, J. A., "Magnetic Stimulation of the Human Brain and Peripheral Nervous System: An Introduction and the Results of an Initial Clinical Evaluation," *Neurosurgery* **20**, 100–109 (1987).

[2] Cohen, L. G., Roth, B. J., Nilsson, J., Dang, N., Panizza, M., et al., "Effects of Coil Design on Delivery of Focal Magnetic Stimulation. Technical Considerations," *Electroencephalogr. Clin. Neurophysiol.* **75**, 350–357 (1990).

[3] Cracco, R.Q., "Evaluation of Conduction in Central Motor Pathways: Techniques, Pathophysiology, and Clinical Interpretation," *Neurosurgery* **20**, 199–203 (1987).

[4] Hess, C. W., Mills, K. R., Murray, N. M. F., and Schriefer, T. N., "Magnetic Brain Stimulation: Central Motor Conduction Studies in Multiple Sclerosis," *Ann. Neurol.* **22**, 744–752 (1987).

[5] Mills, K. R., and Murray, N. M. F., "Corticospinal Tract Conduction Time in Multiple Sclerosis," *Ann. Neurol.* **18**, 601–610 (1985).

[6] Levy, W. J., "Clinical Experience with Motor and Cerebellar Evoked Potential Monitoring," *Neurosurgery* **20**, 169–182 (1987).

[7] Shields, C. B., Edmonds, H. L., Paloheimo, M., Johnson, J. R., and Holt, R. T., "Intraoperative Use of Transcranial Magnetic Motor-Evoked Potentials," in *Proc. 10th Ann. Conf. IEEE-EMBS*, pp. 926–927 (1988).

[8] Day, B. L., Rothwell, J. C., Thompson, P. D., Maertens De Noordhout, A., Nakashima, K., "Delay in the Execution of Voluntary Movements by Electrical or Magnetic Brain Stimulation in Intact Man," *Brain*, **112**, 649–663 (1989).

[9] Amassian, V. E., Cracco, J. B., Cracco, R. Q., Eberle, L., Maccabee, P. J., "Suppression of Visual Perception by Magnetic Coil Stimulation of Human Occipital Cortex," *Electroencephalogr. Clin. Neurophysiol.* **74**, 458–462 (1989).

[10] Cohen, L. G., Roth, B. J., Wassermann, E. M., Topka, H., Fuhr, P., et al., "Magnetic Stimulation of the Human Cerebral Cortex, an Indicator of Reorganization in Motor Pathways in Certain Pathological Conditions," *J. Clin. Neurophys.* **8**, 56–65 (1991).

[11] Maccabee, P. J., Amassian, V. E., Cracco, R. Q., Cracco, J. B., and Anziska, B. J., "Intracranial Stimulation of Facial Nerve in Humans with the Magnetic Coil," *Electroencephalogr. Clin. Neurophysiol.* **70**, 350–354 (1988).

[12] Schriefer, T. N., Mills, K. R., Murray, N. M., and Hess, C. W., "Evaluation of Proximal Facial Nerve Conduction by Transcranial Magnetic Stimulation," *J. Neurol. Neurosurg. Psychiatry* **51**, 60–66 (1988).

[13] Tsuji, S., Murai, Y., and Yarita, M., "Somatosensory Potentials Evoked by Magnetic Stimulation of Lumbar Roots, Cauda Equina, and Leg Nerves," *Ann. Neurol.* **24**, 568–573 (1988).

[14] Chokroverty, S., and DiLullo, J., "Percutaneous Magnetic Stimulation of the Human Lumbosacral Spinal Column: Physiological Mechanism and Clinical Application," *Neurology*, **39**, 376 (1989).

[15] Similowski, T., Fleury, B., Launois, S., Cathala, H. P., Bouche, P., et al., "Cervical Magnetic Stimulation: A New Painless Method for Bilateral Phrenic Nerve Stimulation in Conscious Humans," *J. Appl. Physiol.* **67**, 1311–1318 (1989).

[16] Evans, B. A., Litchy, W. J., and Daube, J. R., "The Utility of Magnetic Stimulation for Routine Peripheral Nerve Conduction Studies," *Muscle & Nerve* **11**, 1074–1078 (1988).

[17] Rank, J. B., "Which Elements Are Excited in Electrical Stimulation of Mammalian Central Nervous System: A Review," *Brain Res.* **98**, 417–440 (1975).

[18] Roth, B. J., and Basser, P. J., "A Model of the Stimulation of a Nerve Fiber by Electromagnetic Induction," *IEEE Trans. Med. Biol. Eng.* **37**, 588–597 (1990).

[19] Reilly, J. P., "Peripheral Nerve Stimulation by Induced Electric Currents: Exposure to Time-Varying Magnetic Fields," *Med. & Biol. Eng. & Comp.* **27**, 101–110 (1989).

[20] Meyer, R. A., Raja, S. N., and Campbell, J. N., "Coupling of Action Potential Activity Between Unmyelinated Fibers in the Peripheral Nerve of Monkey," *Science* **227**, 184–187 (1985).

[21] Ueno, S., Matsuda, T., and Hiwaki, O., "Localized Stimulation of the Human Brain and Spinal Cord by a Pair of Opposing Pulsed Magnetic Fields," *J. Appl. Phys.* **67**, 5838–5840 (1990).

ACKNOWLEDGMENTS: This work was supported by APL biomedical Independent Research and Development funding. The author would like to thank Robert Fisher and Robert W. McPhereson of The Johns Hopkins Medical School for their many insights into problems and applications of magnetic stimulation and for providing the facilities, time, and assistance with the dog experiments. Frank Mark of APL provided valuable assistance in the construction of the stimulator. Richard Meyer, also of APL, provided generous support for the monkey experiments.

THE AUTHOR

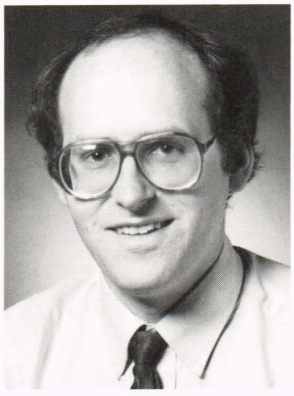

HARRY A. C. EATON received a B.S. degree from Colorado State University in 1985 and an M.S. degree from The Johns Hopkins University in 1990, both in electrical engineering. From 1985 to 1988, he worked in the Submarine Technology Test Group designing various undersea instruments. He joined the Biomedical Programs Office in 1988 and is head of the bioelectromagnetics laboratory at APL. His research interests include analog circuit design, tissue impedance measurement, and magnetic nerve stimulation.